

# Using xanthated *Lagenaria vulgaris* shell biosorbent for removal of Pb(II) ions from wastewater

Miloš Kostić · Miljana Radović · Jelena Mitrović ·  
Milan Antonijević · Danijela Bojić ·  
Milica Petrović · Aleksandar Bojić

Received: 28 February 2013 / Accepted: 27 July 2013 / Published online: 10 August 2013  
© Iranian Chemical Society 2013

**Abstract** Chemically modified *Lagenaria vulgaris* shell was applied as a new sorbent for the removal of lead (II) ions from aqueous solution in a batch process mode. The influence of contact time, initial concentration of lead (II) ions, initial pH value, biosorbent dosage, particle size and stirring speed on the removal efficiency was evaluated. Biosorbent characterization was performed by Fourier transform infrared spectroscopy (FTIR), scanning electron microscopy (SEM) and energy dispersive X-ray spectroscopy (EDX). Four kinetic models (pseudo-first order, pseudo-second order, Elovich model and Intraparticle diffusion model) were used to determine the kinetic parameters. The experimental results were fitted to the Langmuir, Freundlich, Dubinin–Radushkevich and Temkin models of isotherm. Pseudo-second order kinetic model and Langmuir isotherm model best fitted the experimental data. Sorption process is obtained to be fast and equilibrium was attained within 40 min of contact time. The maximum sorption capacity was  $33.21 \text{ mg g}^{-1}$ . Biosorption was highly pH-dependent where optimum pH was found to be 5. The results of FTIR and SEM analysis showed the presence of new sulfur functional groups. This study indicated that xanthated *Lagenaria vulgaris* shell could be used as an effective and low-cost biosorbent for the removal of lead (II) ions from aqueous solution.

**Keywords** Xanthated *Lagenaria vulgaris* · Lead (II) ions · Biosorption · Kinetics

## Introduction

Industrialization and aspiration for industrial growth, on the one hand, and consequences of that industrialization, on the other, have caused great concern about the contamination of environment. This concern is especially prominent in the question of contamination of industrial waste waters by heavy metals: lead, copper, cadmium, zinc, mercury, chromium, etc. Due to their toxic effects on humans, plants, animals and the environment in general, it is very important to explore and investigate different methods and techniques for removing heavy metals from water [1].

Proper and efficient removal of lead is especially important, as this metal can be described as highly toxic (during decades of research no nutritional value or positive biological effect of this metal have been found). Although lead has been used by humans in different applications for many years, it is considered to be a very dangerous poison, particularly for children [2]. Lead is toxic at very low exposure and can cause some serious health problems by affecting nervous, reproductive and immune systems.

Pb(II) can be removed by employing various methods, such as: chemical precipitation, reduction, ion-exchange and electrochemical treatment, which are often expensive or ineffective for reducing Pb(II) ions to very low concentrations [3]. With that in mind, those conventional methods can be replaced with sorption processes, which are among the most effective techniques for the removal of highly toxic metals and which can reduce heavy metal level to environmentally accepted levels at affordable

M. Kostić (✉) · M. Radović · J. Mitrović · D. Bojić ·  
M. Petrović · A. Bojić  
Department of Chemistry, Faculty of Science and Mathematics,  
University of Niš, Višegradska 33, 18000 Niš, Serbia  
e-mail: mk484475@gmail.com

M. Antonijević  
School of Science, University of Greenwich, Chatham Maritime,  
Kent ME4 4TB, UK

costs. Biosorbents based on sulfur-bearing groups (sulfides, thiols, xanthates) have a high-affinity for heavy metals in aqueous solutions, which could be explained in terms of hard and soft acids and bases (HSAB) concept. According to HSAB classification system, sulfur can be considered as a soft ligand group having strong affinity for lead, which is classified as soft acid. The major advantages of biosorption over conventional methods include low cost, high efficiency, minimization of chemical or biological sludge and possibility of biosorbent regeneration.

The objective of this study is to synthesize a novel biosorbent based on xanthated *Legenaria vulgaris* shell (xLVB) and investigate the sorption capabilities for removal of Pb(II) ions from aqueous solutions. The effect of contact time, initial concentration of Pb(II) ions, pH, effect of biosorbent dosage, particle size and effect of stirring speed on Pb(II) ions removal were examined. Moreover, the most often used kinetics and isotherm models as well as various characterization techniques were employed to explain interaction between Pb(II) ions and xanthated *Legenaria vulgaris* biosorbent.

## Experimental

### Reagents

All chemicals were of reagent grade and were used without further refinement.  $\text{HNO}_3$ ,  $\text{NaOH}$ ,  $\text{CS}_2$ ,  $\text{Pb}(\text{NO}_3)_2$  were purchased from Merck (Germany). All solutions were prepared with deionized water (18 M $\Omega$ ). Standard metal stock solution was prepared by dissolving given amounts of  $\text{Pb}(\text{NO}_3)_2$ . All standard solutions were stored in a refrigerator at +4 °C.

### Preparation of xanthated biosorbent

*Legenaria vulgaris* is a creeping, hardy plant, which belongs to the Cucurbitaceae family [4]. It was cultivated and collected from a farm in south Serbia (near the city of Niš). Plant shell was treated with diluted nitric acid and after that by sodium hydroxide, producing a basic *Legenaria vulgaris* biosorbent (LVB) [4]. Xanthation was carried out by the following procedure: 10 g LVB with granulation from 0.8 to 1.25 mm was soaked in 5 mol dm<sup>-3</sup> NaOH, stirred for 90 min and washed with deionized water. This material was then esterified with 1.0 cm<sup>3</sup> of  $\text{CS}_2$  and 50 cm<sup>3</sup> 2.5 mol dm<sup>-3</sup> NaOH for another 3 h. Xanthated material (xLVB) was allowed to settle for 1 h and was separated by decantation and filtration. After that, biosorbent was washed with deionized water, dried at 40 °C and stored in an airtight plastic container for further use. Obtained biosorbent assumed the

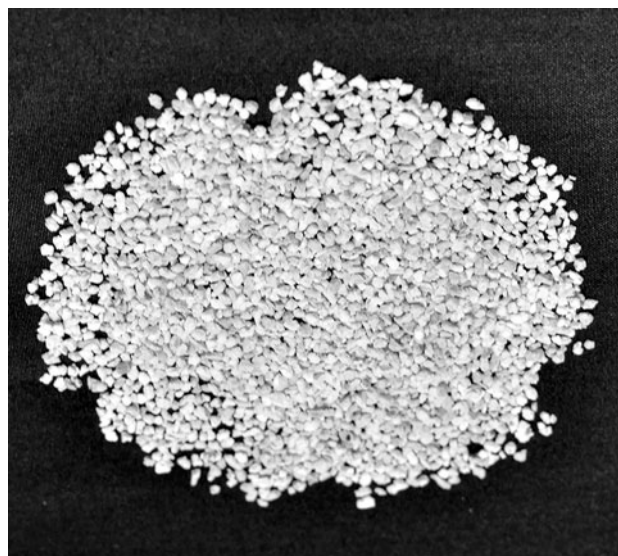


**Fig. 1** Xanthated *Legenaria vulgaris* biosorbent (xLVB)

form of solid porous granules, with a regular uniform shape, which does not swell and does not significantly change its volume in contact with water (Fig. 1), by which it is similar with expensive commercial ion-exchange resins. During the treatment of aqueous solutions biosorbent can be easily separated from the water phase by decantation and filtration and unlike other natural materials (orange peel, rice straw, sugarcane bagasse etc.) [5] does not change the consistency and particle dimensions because of stirring.

### Batch biosorption experiments

Working solutions with the desired concentrations of Pb(II) ions were obtained by proper dilutions of the stock solution (1.00 g dm<sup>-3</sup>) with deionized water. pH of the aqueous metal solution was adjusted using 0.1/0.01 mol dm<sup>-3</sup> NaOH/HNO<sub>3</sub> (SensIon5, HACH, USA). Typical sorption experiments were performed with 250 cm<sup>3</sup> of solutions, containing different Pb(II) ions concentrations (from 10.0 to 400.0 mg dm<sup>-3</sup>), different biosorbent dose (from 0.5 to 8.0 g dm<sup>-3</sup>) and at determined pH value. The influence of the initial pH was examined at the pH values ranging from 2.0 to 6.0 (maintained during treatment within the limits of  $\pm 0.2$ , without buffering), while all other parameters were kept constant. The parallel experiment was a blank system, a treatment of the same solution without biosorbent. The blank system was used for testing the loss of metal on glass dishes. Residual Pb(II) ions concentrations in all samples were measured using air-acetylene flame atomic absorption spectrometer AAnalyst 300 (Perkin Elmer, USA).

The amount of biosorption  $q_t$  ( $\text{mg g}^{-1}$ ) was calculated by the following equation:

$$q_t = \frac{(c_0 - c_t)V}{m} \quad (1)$$

where  $c_0$  and  $c_t$  are the initial and final concentrations of the metal ions in the solution ( $\text{mg dm}^{-3}$ ),  $V$  is the solution volume ( $\text{dm}^3$ ) and  $m$  is the mass of the sorbent (g).

The removal efficiency (RE) was calculated using the equation:

$$\text{RE (\%)} = \frac{c_0 - c_t}{c_0} \times 100 \quad (2)$$

where  $c_0$  and  $c_t$  are the initial and final concentrations of the metal ions in the solution ( $\text{mg dm}^{-3}$ ).

All the adsorption experiments were conducted in triplicate, and the mean values were calculated. The results were reproducible at most 5 % error. Statistical analysis, calculation of the data and linear least square fitting were carried out using OriginPro 8.0 (OriginLab Corporation, USA) software.

#### Characterization of the sorbent

The FTIR spectra of untreated, xanthated and Pb loaded biosorbents were carried out as a qualitative analysis to determine the main functional groups present in the sorbent and their changes after metal solution treatment. For those purposes the Bomem Hartman and Braun MB-100 spectrometer was used and the samples were prepared as KBr pellets under high pressure.

The morphology of xLVB minor surface was analyzed by scanning electron microscopy (SEM) at  $500 \times$  and  $1,000 \times$  magnification. Samples were stuck onto aluminum stubs using Leit-C carbon cement and then carbon coated in an Edwards 306 high-vacuum carbon evaporator to ensure surface conductivity for EDX. Secondary electron images were taken using the lower detector of a Hitachi SU8030 cold-cathode field emission gun scanning electron microscope (FEG-SEM) at 2 kV accelerating voltage, at various working distances between 10 and 16 mm.

Energy Dispersive X-ray microanalysis (EDX) was performed using a Thermo-Noran NSS system 7 with a  $30 \text{ mm}^2$  window Ultra Dry detector. The working distance was fixed at 15 mm and an accelerating voltage of 10 kV was chosen to give adequate excitation of the K lines of the lighter elements, the L lines of Cu, Cd and Ni, and the M lines of Bi and Pb while limiting the beam damage to the sample. Three replicated analyses were taken within a single field of view.

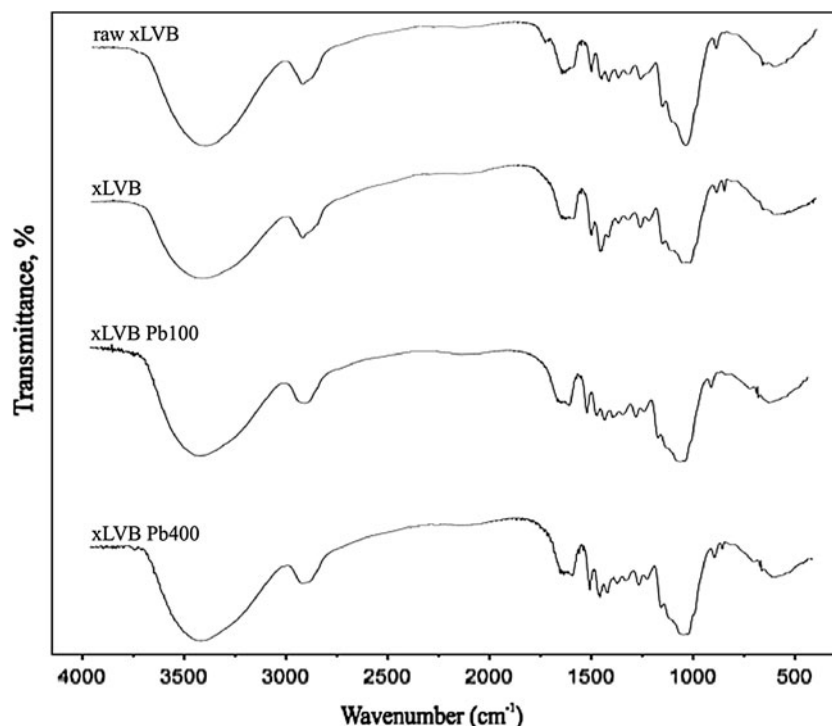
## Results and discussion

### Fourier transform infrared spectroscopy (FTIR) analysis

The FTIR spectra of untreated (LVB), xanthated (xLVB) and loaded biosorbents with two initial Pb(II) concentrations (initial Pb(II) xLVB Pb100 and xLVB Pb400) were taken to obtain information on the nature of surface functional groups and the possible biosorbent–lead(II) ions interactions (Fig. 2). The broad and intense band presented in the spectrum of untreated LVB centered around  $3,416 \text{ cm}^{-1}$ , corresponds to the O–H stretching vibrations. This band is a consequence of the inter- and intra-molecular hydrogen bonding of polymeric compounds such as alcoholic, phenolic and carboxylic groups, which are characteristic for cellulose and lignin, the main constituents of *Lagenaria vulgaris* shell [6]. The peak at  $2,925 \text{ cm}^{-1}$  is attributed to the symmetric and asymmetric C–H stretching vibration of aromatic methoxyl groups and to methyl and methylene groups of side chains [7]. The peak observed at  $1,735 \text{ cm}^{-1}$  is the stretching vibration of C = O bond due to non-ionic carboxyl groups ( $-\text{COOH}$ ,  $-\text{COOCH}_3$ ), and may be assigned to carboxylic acids or their esters. Asymmetric and symmetric stretching vibrations of ionic carboxylic groups ( $-\text{COO}^-$ ) appeared at  $1,637$  and  $1,458 \text{ cm}^{-1}$ . Aromatic ring bands appeared at  $1,507 \text{ cm}^{-1}$ , the band that appeared at  $1,420 \text{ cm}^{-1}$  is the stretching characteristic vibration for lignin, the bending vibration of OH at  $1,328 \text{ cm}^{-1}$  has been reported for syringyl ring of hardwood and non-wood lignins [8]. Moreover, intense band at  $1,048 \text{ cm}^{-1}$  can be connected to the existence of stretching vibration of C–OH of alcoholic groups and already registered carboxylic acids [9]. Some distinct changes are noted in the FTIR spectrum of LVB, xLVB, xLVB Pb100 and xLVB Pb400 biosorbents. The broad peak obtained in untreated biosorbent at  $3,416 \text{ cm}^{-1}$  was shifted to  $3,413$ ,  $3,425$  and  $3,421 \text{ cm}^{-1}$  in the xLVB, xLVB Pb 100 and xLVB Pb 400, respectively. These findings indicating that the hydroxyl group can be involved in the sorption process. Furthermore, FTIR spectra of untreated biosorbent, xLVB, Pb(II)-sorbed xLVB showed that the peaks expected at  $1,048 \text{ cm}^{-1}$  were shifted to  $1,061 \text{ cm}^{-1}$  for xLVB,  $1,064 \text{ cm}^{-1}$  for xLVB Pb100 and to  $1,065 \text{ cm}^{-1}$  for xLVB Pb400. These findings indicates that the hydroxyl group from carboxylic acids was involved in metal biosorption. Moreover, the peak centered at  $1,025 \text{ cm}^{-1}$  in FTIR spectrum of xLVB, corresponding to the C = S stretching vibrations, was shifted to  $1,028 \text{ cm}^{-1}$  in case of xLVB Pb100 and to  $1,027 \text{ cm}^{-1}$  in case of xLVB Pb400.

The presence of sulfur groups in the xLVB has been identified by the appearance of new peaks at  $534$ ,  $1,026$ ,

**Fig. 2** FTIR spectra of untreated biosorbent material and xLVB before and after Pb(II) adsorption treatment



1,159 and 1,227  $\text{cm}^{-1}$  corresponding to C–S, C = S, S–C–S and O = C=O [6]. In addition, the elementary analysis of xLVB provided important increase of S element content ( $17.44 \text{ mg g}^{-1}$ ) compared to untreated material ( $0.19 \text{ mg S g}^{-1}$ ), which together with above mentioned new peaks in FTIR spectrum confirmed that the incorporation of sulfur groups on surface of biomaterial and xanthation was successful. The results of FTIR analysis indicated that the functional groups, such as hydroxyl, carboxylic and C = S presented in untreated biosorbent, xLVB and Pb(II)-sorbed xLVB, participated in the sorption of Pb(II) ions and provide the better understanding of sorption mechanism.

#### Scanning electron microscopy (SEM) and energy dispersive X-ray spectroscopy (EDX) analysis

The morphological characteristics of the biomass surface were examined by scanning electron microscopy. The presence of voids on the surface of xLVB biosorbent revealed the possibility of Pb(II) ion accumulation (Fig. 3). The surface was not smooth; rough surface texture and porosity could be distinctly noticed.

EDX analysis of xLVB biosorbent before and after biosorption Pb(II) ions has been represented in Figs. 4 and 5. The presence of peaks of S and Na (Figs. 4, 5), recorded in the modified biosorbent, with FTIR results, confirms the anchoring of xanthate group on the biosorbent surface with regard to basic material (results not shown). The EDX

spectrum for xLVB, before the sorption of Pb(II) ions, did not show the characteristic signal of Pb(II) ions (Fig. 4), whereas for the Pb(II) loaded xLVB (Fig. 5) a clear signal of the presence of Pb(II) ions was observed. EDX analysis provided direct evidence for the sorption of lead onto xLVB. Furthermore, sodium, which is capable of ion-exchange with Pb(II) ions, was present at high concentration. After the sorption of the Pb(II) ions onto xLVB, the concentration of sodium was high decreased from 2.86 to 0.71 % in the EDX spectrum of Pb(II) ions loaded xLVB, thus suggesting the ion-exchange process.

#### Contact time effect

To investigate the effect of contact time 1 g of xLVB was added to  $250 \text{ cm}^3$  of Pb(II) solution with concentration of  $50 \text{ mg dm}^{-3}$  and at pH 5. As one can notice from Fig. 6 sorption of Pb(II) ions occurred in two stages; initial faster and subsequent slower. The initial fast phase is likely to occur because of high-availability of active binding sites on the sorbent surface (diffusion process) [10]. Further, increase in contact time did not show a significant decreasing of Pb(II) concentration, owing to the fact that diffusion of the lead ions into the inner part of the biosorbent took place. Furthermore, the experimental results revealed high-biosorbent efficiency for removing Pb(II) ions, whereas maximum adsorption efficiency was obtained in the first 20 min of sorbent–sorbate contact. In this period, 90.96 % of total Pb(II) ions were removed and the sorption capacity ( $q_t$ ) was  $9.64 \text{ mg g}^{-1}$ . The

sorption equilibrium was attained after about 40 min of contact time. In the state of equilibrium,  $q_t$  was  $10.26 \text{ mg g}^{-1}$ , 98.67 % of total Pb(II) ions were removed from aqueous solution and initial concentration of Pb(II) ions decreased from  $50.0$  to  $0.569 \text{ mg dm}^{-3}$ . To the end of the treatment, changes of metal concentrations in the solution were

negligible. After 180 min of treatment,  $q_t$  was  $10.48 \text{ mg g}^{-1}$  (RE 98.87 %). Therefore, an optimum contact time of 20 min is sufficient to achieve significant Pb(II) ions removal efficiency; however, a higher contact period (40 min) may be necessary to ensure that equilibrium is established.

Effect of initial Pb(II) concentration

Biosorption of metal ions by any biosorbent is highly dependent on the initial concentration of metal ions. Moreover, it is important to examine this specific parameter owing to the fact that wastewater from various processes usually contain metal ions in a wide range of concentrations. The effect of various initial Pb(II) ions concentrations ( $10, 20, 50, 100, 200$  and  $400 \text{ mg dm}^{-3}$ ) on sorption was investigated with all other parameters keeping constant (xLVB dose  $4.0 \text{ g dm}^{-3}$ , pH 5 and the temperature of  $25.0 \pm 0.5 \text{ }^\circ\text{C}$ ). The results showed that by increasing initial metal ions concentration from  $10$  to  $400 \text{ mg dm}^{-3}$ , the loading capacity of the sorbent increased from  $2.47$  to  $33.05 \text{ mg}$  of Pb(II) per gram of xLVB (Fig. 7). In the case of low initial Pb(II) concentrations  $10, 20$  and  $50 \text{ mg dm}^{-3}$  removal efficiency attains 100 %. For initial Pb(II) concentration of  $100 \text{ mg dm}^{-3}$  removal efficiency reached 91 %, while at higher concentrations  $200$  and  $400 \text{ mg dm}^{-3}$  removal efficiency decreased to 63 and 32 %, respectively. Sorption capacity,  $q_e$ , linearly increased with increasing Pb(II) ions concentration to  $200 \text{ mg dm}^{-3}$ , after which saturation occurs. In other words, with increasing metal ions concentration above  $200 \text{ mg dm}^{-3}$  the percentage of metal removal decreased due to diminishing loading capacity of biosorbent since that the binding sites are limited by keeping biosorbent loadings constant [11].

Effect of biosorbent dosage

The effect of variation in the sorbent dose from  $0.5$  to  $8 \text{ g dm}^{-3}$  on the sorption of Pb(II) ions at constant values of pH, sorbate concentration and stirring speed  $200 \text{ rpm}$

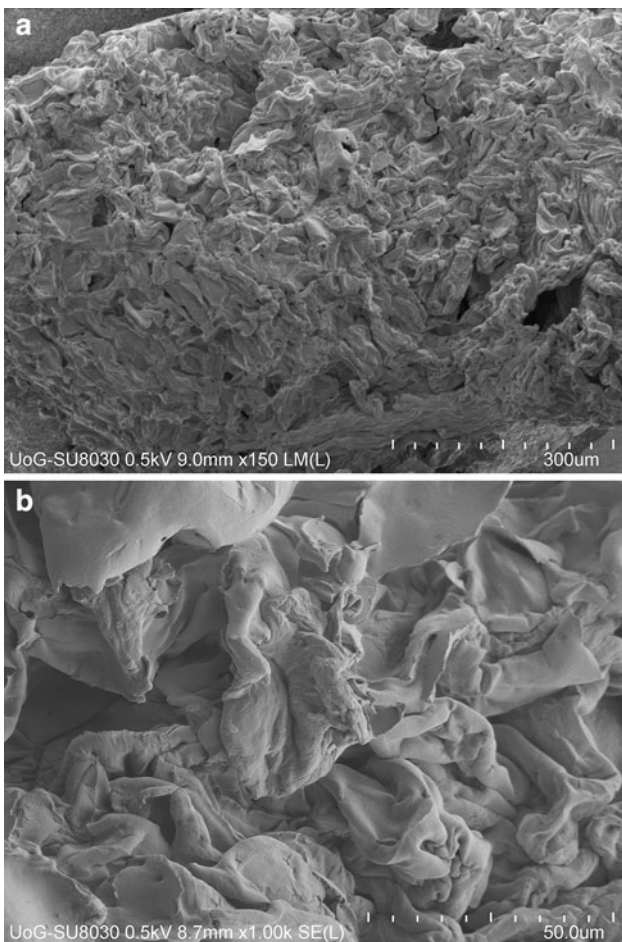


Fig. 3 Scanning electron micrographs of a xLVB 150 × magnification and b 1,000 × magnification

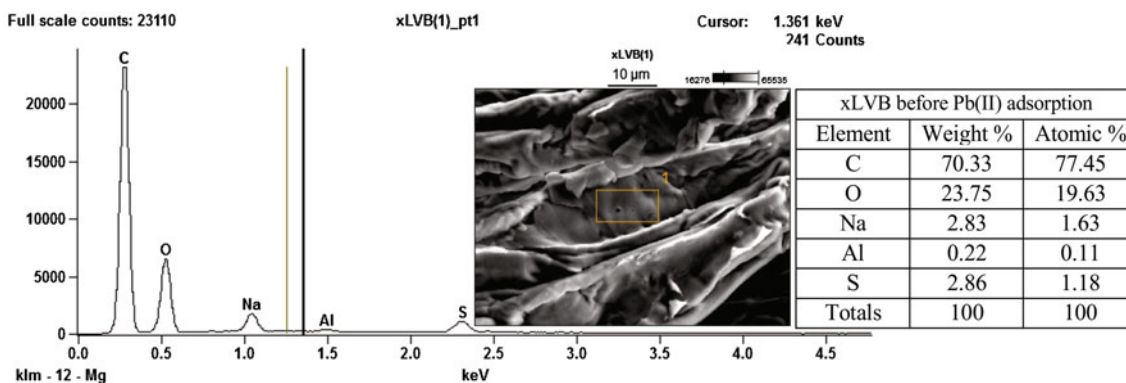
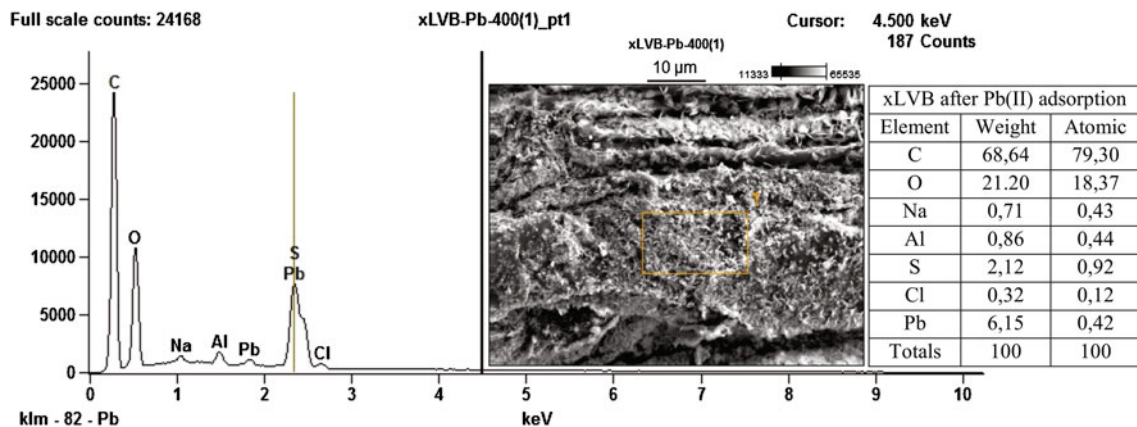
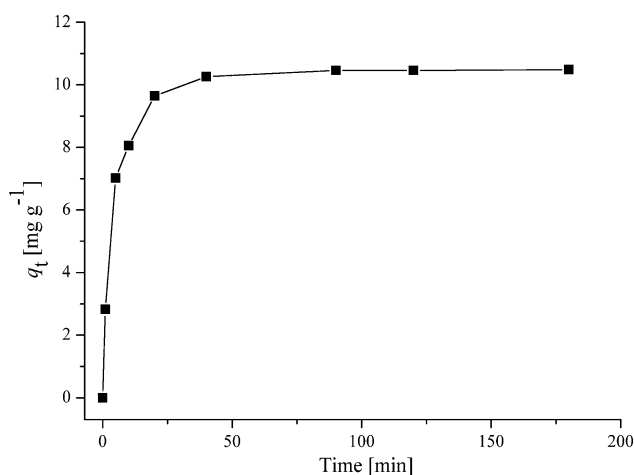


Fig. 4 SEM at 2,000 × magnification and EDX spectra of xLVB before adsorption



**Fig. 5** SEM at 2,000 × magnification and EDX spectra of xLVB after adsorption



**Fig. 6** Removal of Pb(II) ions from aqueous solutions by xLVB. Initial pH was 5,  $[\text{Pb(II)}]_0 = 50.0 \text{ mg dm}^{-3}$ , sorbent dose was  $4.0 \text{ g dm}^{-3}$ , temperature was  $25.0 \pm 0.5 \text{ }^\circ\text{C}$  and stirring speed 200 rpm

were studied. Removal efficiency of Pb(II) ions was low at lower doses ( $0.5, 1 \text{ g dm}^{-3}$ ) and gradually increased with increasing in biosorbent doses ( $2, 4 \text{ g dm}^{-3}$ ) as it is presented in Fig. 8. This can be attributed to the fact that the more mass available, the more the contact effective surface area offered to the sorption. The maximum Pb(II) adsorption (99.83 %) was achieved with a biosorbent concentration of  $4.0 \text{ g dm}^{-3}$ . A further increase in sorbent dosage up to  $8 \text{ g dm}^{-3}$  smoothly declined removal efficiency to 97.86 %, which probably can be ascribed to the overlapping or aggregation of sorption sites and decreasing in total sorbent surface area.

#### Effect of particle size

The effect of altering the sorbents particle size on the removal efficiency is shown in Fig. 9. Experimental data indicated that the removal of Pb(II) ions was increased from

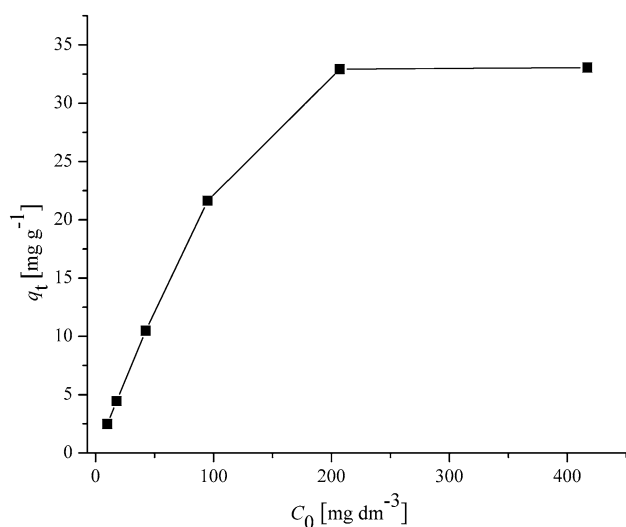


**Fig. 7** Effect of the initial concentration on the adsorption of Pb(II) onto xLVB. Initial pH 5,  $[\text{Pb(II)}]_0 = 50.0 \text{ mg dm}^{-3}$ , sorbent dose was  $4.0 \text{ g dm}^{-3}$ , temperature was  $25.0 \pm 0.5 \text{ }^\circ\text{C}$  and stirring speed 200 rpm

85.2 to 99.91 % by decreasing the particle sizes from 2.5–4.0 mm to  $< 0.4 \text{ mm}$ . This behavior can be attributed to the effective surface area, which increased as the particle size decreased and, as a consequence, Pb(II) ions sorption increased. The particle size 0.8–1.25 mm was selected for further study because the particle sizes of 0.4–0.8 mm and less than 0.4 mm were too small and difference in removal efficiency was insignificant. On the other hand, sorbents with higher particle size (1.25–2.5 mm and 2.5–4.0 mm) were shown to be less efficiency than sorbents with particle size from 0.8 to 1.25 mm because of lower effective surface area.

#### Effect of stirring speed on Pb(II) ions biosorption

The effect of stirring speed on removal efficiency of Pb(II) ions was investigated in the range from 100 to 600 rpm. The influence of the stirring speed on the removal

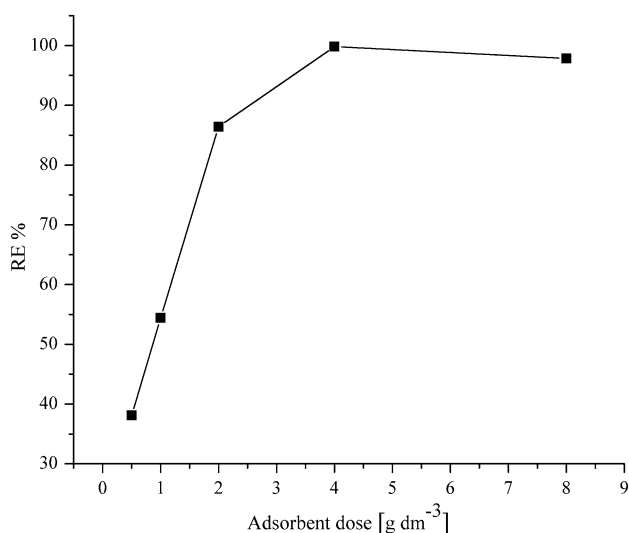


**Fig. 8** Effect of adsorbent dose on Pb(II) ions removal with xLVB. Initial Pb(II) ions concentration  $50 \text{ mg dm}^{-3}$ , pH  $5.0 \pm 0.1$ , contact time 180 min, temperature was  $25.0 \pm 0.5 \text{ }^\circ\text{C}$  and stirring speed 200 rpm

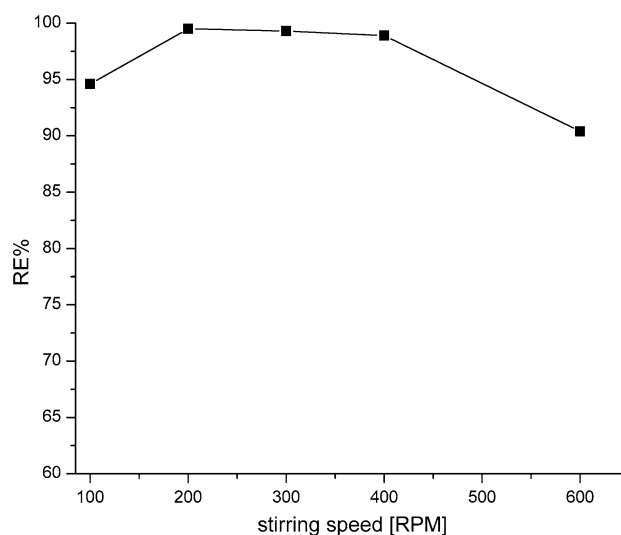


**Fig. 10** Effect of stirring speed on the removal efficiency (RE) of xLVB. Experimental conditions: pH 5, sorbent dose  $4.0 \text{ g dm}^{-3}$ , initial metal concentration  $50 \text{ mg dm}^{-3}$ , contact time 180 min, temperature was  $25.0 \pm 0.5 \text{ }^\circ\text{C}$

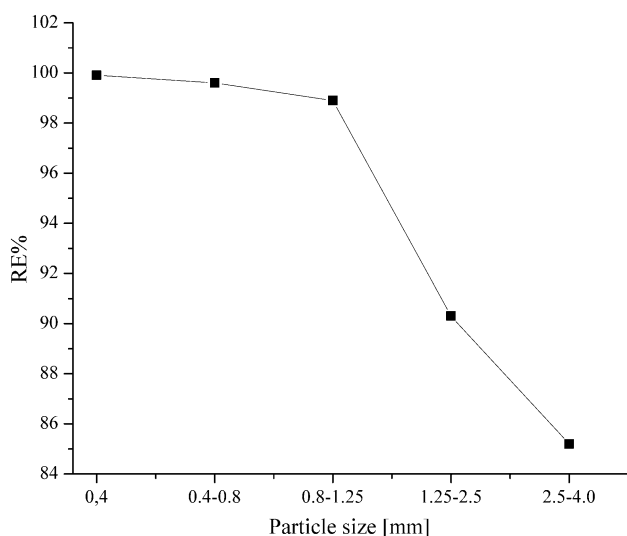


**Fig. 9** Effect of biosorbent particle size on uptake of Pb(II) from aqueous solutions by xLVB. Experimental conditions: pH 5, sorbent dose  $4.0 \text{ g dm}^{-3}$ , initial metal concentration  $50 \text{ mg dm}^{-3}$ , contact time 180 min, temperature was  $25.0 \pm 0.5 \text{ }^\circ\text{C}$  and stirring speed 200 rpm

efficiency of the biosorbent showed that an optimum value was obtained at 200 rpm (Fig. 10). This stirring speed was used in all our experiments. xLVB has a low specific weight, and floats on the surface in contact with the solution. The increase in stirring speed from 100 to 200 rpm resulted in an increase of removal efficiency of Pb(II) ion (from 94.6 to 99.5 %). Increasing stirring rate reduces the film boundary layer surrounding the sorbent particles, thus increasing the external film mass transfer coefficient and

the rate of adsorption Pb(II) ions. In range of 200–400 rpm removal efficacy is almost without change. By increasing the speed further from 400 to 600 rpm, decreased of removal efficiency from 98.9 to 90.4 % was obtained. At high stirring speed, vortex phenomena occurs and the suspension was no longer homogenous which makes the sorption of Pb(II) ions difficult.

#### Effect of initial pH

Solution pH is the most important variable governing the sorption of metal ions by the sorbent [12]. The influence of the initial pH was examined at a different pH ranging from 2.0 to 6.0, with the xLVB dose of  $4.0 \text{ g dm}^{-3}$  and at temperature  $25.0 \pm 0.5 \text{ }^\circ\text{C}$ . The results (Fig. 11) indicated that relatively little biosorption took place at the initial pH 2 and about 34.05 % of Pb(II) ions were removed. A continuous increase in the sorption capacity of xLVB occurred in the pH range of 2–5 (99.73 % Pb(II) ions at pH 5.0), and then it slightly decreased to 99.28 % at pH 6.0. Basic material from which xLVB on pH 2 was obtained had RE 6.8 %, so pH had more significant influence on the basic material than on xLVB. Those results are not shown.

pH influences metal ion sorption due to the competition between the metal and  $\text{H}^+$  ions for active sorption sites [13]. The minimum biosorption at low pH 2.0 may be due to the high concentration and high mobility of  $\text{H}^+$  ions, whereas the hydrogen ions are preferentially sorbed rather than the metal ions. At higher pH values, the lower number of  $\text{H}^+$  and greater number of ligands with negative charges result in greater metal ions biosorption. As the solution pH

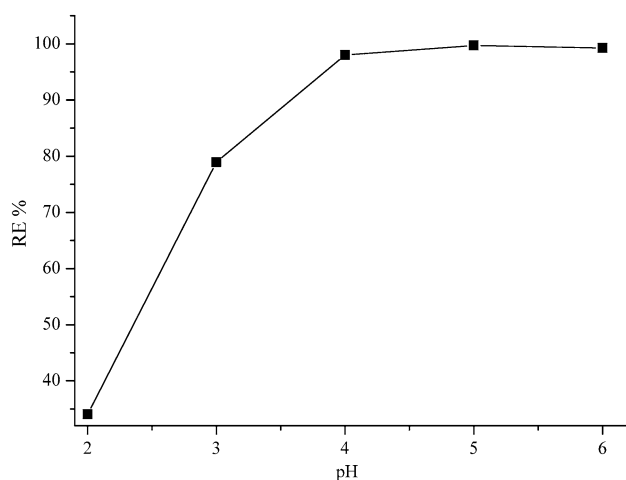
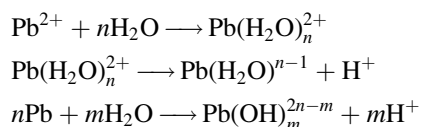


**Fig. 11** Effect of initial pH on the removal efficiency of Pb(II) ions.  $[\text{Pb(II)}]_0 = 50.0 \text{ mg dm}^{-3}$ , sorbent dose was  $4.0 \text{ g dm}^{-3}$ , temperature was  $25.0 \pm 0.5 \text{ }^\circ\text{C}$  and stirring speed 200 rpm

was increased, the ability of Pb(II) ions for competition with  $\text{H}^+$  ions was also increased, but at pH 6.0 enhanced metal removal from the solution could be, partly, a result of metal hydroxide precipitation [14]. The results suggest that the biosorption of Pb(II) ions to the xLVB is mainly due to electrostatic attraction [11]. The pH speciation shows that the dominant species is  $\text{Pb(OH)}_2$  at  $\text{pH} > 5$  and  $\text{Pb}^{2+}$  and  $\text{Pb(OH)}^+$  at  $\text{pH} < 5$  [13].



For this reason, further metal sorption studies were carried out at pH 5.0, which is well below the pH levels where Pb(II) ions are precipitated. The adsorption capacity of xLVB at pH in the range of 4–6 was about  $12.4 \text{ mg g}^{-1}$ . The adsorption capacities of xLVB as a function of the initial pH are presented in Fig. 12. Above pH 6.0, insoluble lead hydroxide starts precipitating from the solution. The effect of pH can be explained by considering the surface charge on the sorbent material. The zero charge of the sorbent, which is the point at which the net charge of the sorbent is zero, was determined as 7.8. The pH of point of zero charge measurement on this sorbent supports this observation, below which the surface is net positively charged and unable to bind  $\text{Pb}^{2+}$  ions. Generally, the net positive charge decreased with increasing pH value and led to decrease in the repulsion between the sorbent surface and metal ions and thus, enhanced the adsorption capacity. The basic material LVB, from which xLVB at pH 2.0 was obtained has RE 10.2 % (results not shown), which indicated that initial pH has much smaller influence on xLVB, because of presence of strong acid xantate groups

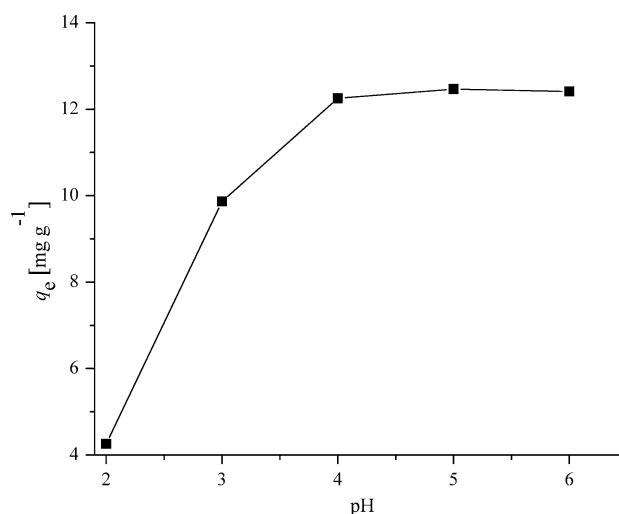


**Fig. 12** Effect of pH on the adsorption of Pb(II) ions onto xLVB.  $[\text{Pb(II)}]_0 = 50.0 \text{ mg dm}^{-3}$ , sorbent dose was  $4.0 \text{ g dm}^{-3}$ , temperature was  $25.0 \pm 0.5 \text{ }^\circ\text{C}$  and stirring speed 200 rpm

that are difficult to protonated. These negative groups have high-affinity for the binding of positive charged metal ions, even at a relatively low pH, probably by means of the ion-exchange mechanism.

#### Sorption isotherms

Sorption isotherms can be defined as the distribution of metal ions between the biosorbent and the metal solution, in the state of equilibrium. A sorption isotherm provides information important for designing an optimal biosorption system, biosorption mechanism and information about capacities of biosorbents. The sorption process is described by four widely used isotherms: Langmuir, Freundlich, Temkin and Dubinin–Radushkevich isotherm.

Langmuir adsorption isotherm is the most widely used model for the sorption process and it is based on homogeneous surface by monolayer coverage of adsorbate on the surface of sorbents [15]. The Langmuir equation can be expressed as:

$$\frac{c_e}{q_e} = \frac{c_e}{q_{\max}} + \frac{1}{q_{\max}K_L}$$

where  $q_e$  ( $\text{mg g}^{-1}$ ) is the amount of metal removed per gram of sorbent,  $q_{\max}$  ( $\text{mg g}^{-1}$ ) is the maximum sorption capacity,  $C_e$  ( $\text{mg dm}^{-3}$ ) is concentration in the equilibrium solution, and  $K_L$  ( $\text{mg dm}^{-3}$ ) is the Langmuir constant related to the adsorption energy.

The value of separation factor indicates the type of the isotherm and the nature of the adsorption process. Considering the  $R_L$  value, adsorption can be unfavorable ( $R_L > 0$ ), linear ( $R_L = 1$ ), favorable ( $0 < R_L < 1$ ) or irreversible ( $R_L = 0$ ).

$$R_L = \frac{1}{1 + K_L c_0}$$

Freundlich isotherm model best applies to adsorption on heterogeneous surfaces [16]. Freundlich isotherm can be expressed as follows:

$$\log q_e = \frac{1}{n} \log c_e + \log K_F$$

where  $q_e$  is the equilibrium sorption concentration of solute per gram of adsorbent ( $\text{mg g}^{-1}$ ),  $C_e$  is the equilibrium aqueous concentration of the solute ( $\text{mg dm}^{-3}$ ),  $K_F$  and  $n$  are Freundlich constants which are related to the adsorption capacity and the intensity of sorption. The plot of  $\log q_e$  versus  $\log C_e$  has a slope with the value of  $1/n$  and an intercept value of  $\log K_F$ .

The Temkin isotherm [17] assumes that the heat of adsorption of all the molecules in the layer decreases linearly with coverage due to adsorbent–adsorbate interactions rather than logarithmic [18], and that the adsorption is characterized by a uniform distribution of the binding energies, up to some maximum energy. The Temkin isotherm can be expressed as follows:

$$q_e = B \ln K_t + B \ln c_e$$

where  $K_t$  ( $\text{dm}^3 \text{mg}$ ) is the equilibrium binding constant corresponding to the maximum binding energy and constant  $B = RT/b$  represents the heat of adsorption, while  $R$  is the universal gas constant ( $8.314 \text{ J mol}^{-1} \text{ K}^{-1}$ ),  $T$  is the absolute temperature in Kelvin and  $1/b$  indicates the adsorption potential of the sorbent.

The Dubinin–Radushkevich model was chosen to estimate the characteristic porosity and the apparent free energy of adsorption. Another equation that has been used to determine the possible biosorption mechanism is the Dubinin–Radushkevich equation, which assumes a constant sorption potential. The linear form of the D–R isotherm equation [19] is:

$$\ln q_e = \ln q_{\text{DR}} - k_{\text{DR}} \varepsilon^2$$

where  $q_e$  is the amount of metal ions sorbed per unit weight of biosorbent ( $\text{mg g}^{-1}$ ),  $q_{\text{DR}}$  is the maximum biosorption capacity ( $\text{mg g}^{-1}$ ),  $k_{\text{DR}}$  is the activity coefficient related to biosorption mean energy ( $\text{mol}^2 \text{kJ}^{-2}$ ) and  $\varepsilon$  is the Polanyi potential described as

$$\varepsilon = RT \ln \left( 1 + \frac{1}{c_e} \right)$$

where  $C_e$  is the equilibrium concentration of the Pb(II) in solution ( $\text{mg dm}^{-3}$ ),  $R$  is the gas constant ( $8.314 \text{ J mol}^{-1} \text{ K}^{-1}$ ), and  $T$  is the temperature ( $K$ ).

The approach was usually applied to distinguish the physical and chemical adsorption of metal ions [20], with

its mean free energy,  $E$  per molecule of adsorbate (for removing a molecule from its location in the sorption space to the infinity) can be computed by the relationship [21]:

$$E = \frac{1}{\sqrt{2k_{\text{DR}}}}$$

where  $E$  ( $\text{kJ mol}^{-1}$ ) gives information about the physical and chemical features of sorption.

All values for isotherm model parameters are given in Table 1. The sorption characteristic of Pb(II) ions on the functionalized xLVB follows the most closely the Langmuir isotherm model. The  $R_L$  values were found to be less than 1 and greater than 0 for all experiments carried out at different initial concentrations. The values of  $R_L$  at 25 °C for sorption of Pb(II) ions by xLVB decreased from 0.117 to 0.0031, while the initial concentration of Pb(II) concentration increased from 10 to 400  $\text{mg dm}^{-3}$ . These results show that Pb(II) ions sorption on xLVB is more favorable at the higher Pb(II) concentration.

The  $r^2$  and  $q_{\text{max}}$  values suggested that the Langmuir isotherm described the sorption process the best as compared to the models of Freundlich, Temkin and Dubinin–Radushkevich. Uptake of Pb(II) ions occurs on a homogeneous surface by monolayer adsorption without any interaction between sorbed ions. The absence of interactions between sorbed ions indicates that the chemical mechanism of sorption probably prevails. The maximum sorption capacity ( $q_{\text{max}}$ ) for Pb(II) ions on xLVB amounts to 33.21  $\text{mg g}^{-1}$ . The differences in sorption capabilities of xLVB and basic *Lagenaria vulgaris* may be due to different functional groups. Since the xanthate group can be classified as soft bases according to the HSAB theory, xanthated biosorbent will certainly show a much higher adsorption capacity in comparison with that of basic

**Table 1** Equilibrium model parameters for adsorption of Pb(II) ions onto xLVB

Equilibrium model	Parameter	Value
Langmuir isotherm	$K_L$ ( $\text{dm}^3 \text{mg}^{-1}$ )	0.763
	$q_{\text{max}}$ ( $\text{mg g}^{-1}$ )	33.212
	$r^2$	0.99973
Freundlich isotherm	$K_F$ ( $\text{dm}^3 \text{g}^{-1}$ )	10.492
	$n$	4.013
	$r^2$	0.94779
Temkin isotherm	$K_t$	1.005
	$B$ ( $\text{kJ mol}^{-1}$ )	0.78
	$r^2$	0.96776
Dubinin–Radushevich	$q_{\text{DR}}$	23.3078
	$E$	5.351
	$k_{\text{DR}}$	$1.7462 \times 10^{-8}$
	$r^2$	0.85441

biosorbent [22]. Basic *Lagenaria vulgaris* biosorbent has predominantly carboxyl and hydroxyl groups as binding ligands for lead which are characterized as hard bases. Therefore, the affinity and sorption capabilities of basic *Lagenaria vulgaris* are lower for heavy metals, compared to xLVB. The correlation coefficients in respect to sorption of Pb(II) ions come out to be 0.9997, 0.9677, 0.9477 and 0.8544 for Langmuir, Temkin, Freundlich and Dubinin–Radushkevich models, respectively.

The Freundlich constant,  $n$ , is a measure of the deviation of the adsorption from linearity. If the value of  $n$  is equal to unity, the adsorption is linear. If the value of  $n$  is below unity, it implies that the sorption process is unfavorable and if the value of  $n$  is above unity, sorption is favorable. In the present study, the value of  $n$  for xLVB at equilibrium was above unity, suggesting favorable sorption. In the experiment that was carried out, the value of  $n$  was higher than 4. Reed and Matsumoto [23] have pointed out that the situation  $n > 1$  is the most common and may be due to a distribution of surface sites or any factor that causes a decrease in adsorbent–adsorbate interaction with increasing surface density. According to McKay et al. [24] the values of  $n$  in the range of 2–10 represent good adsorption. In conclusion, xLVB has a good affinity for Pb(II) ions.

The Temkin adsorption potential,  $K_t$ , of xLVB for Pb(II) ions is 1.005, indicating high-biosorbent metal ion potential for Pb(II) probably due to its large ionic radius. The Temkin constant,  $B$ , related to the heat of sorption for the Pb(II) ions was  $0.78 \text{ kJ mol}^{-1}$ , indicating that interactions between the sorbate and sorbent are neither purely ion-exchange nor purely physisorption [25].

From Dubinin–Radushkevich model it can be seen that the mean sorption energy ( $E$ ) was evaluated to be  $5.351 \text{ kJ mol}^{-1}$  for the biosorption of Pb(II) at temperature  $25 \text{ }^\circ\text{C}$ . According to the literature, the  $E$  value ranges from  $1.0$  to  $8.0 \text{ kJ mol}^{-1}$  are characteristic for physical adsorption and from  $9.0$  to  $16.0 \text{ kJ mol}^{-1}$  for chemical and ion-exchange adsorption [26–28]. Hence, sorption of Pb(II) ions onto xLVB may be attributed to the physical adsorption. The correlation coefficient for Dubinin–Radushkevich model is low (0.8544), so that this model could not be applied for describing the sorption of Pb(II) onto xLVB. A comparative assessment of Pb(II) with various other sorbents reported in the literature revealed the high efficiency of the developed sorbent (Table 2). The differences in sorption capabilities of individual biological materials may be due to different surface characteristics, associated with the presence of different functional groups.

#### Kinetic study

Kinetic studies of metal adsorption by the xLVB were conducted to determine the minimum time to achieve the

sorption equilibrium and to try to explain process mechanism. Lagergren's first-order kinetic model and Ho's pseudo-second order model are the most frequently used in the literature to predict the mechanism involved in the sorption process [7, 37]. In addition to these two models, two more models have been used in this paper: the Elovich model and the intraparticle diffusion model.

The pseudo-first order model was proposed by Lagergren in 1898 [38]. This model describes the rate of sorption to be proportional to the number of sites unoccupied by the solutes. The logarithmic form is:

$$\ln(q_e - q_t) = \ln q_{DR} - kt$$

where  $q_e$  ( $\text{mg g}^{-1}$ ) is the mass of metal ions sorbed at equilibrium,  $q_t$  ( $\text{mg g}^{-1}$ ) is the mass of metal sorbed at time  $t$ , and  $k$  ( $\text{min}^{-1}$ ) is the pseudo-first order reaction rate equilibrium constant. A straight line of  $\ln(q_e - q_t)$  versus  $t$  indicates application of the pseudo-first order kinetics model (Fig. 13), where, in a true pseudo-first order process,  $\ln q_e$  should be equal to the intercept and  $k$  equal to the slope of plot of  $\ln(q_e - q_t)$  against  $t$ , respectively.

The kinetics of the sorption process may also be described using a pseudo-second order rate equation. The linearized form of the equation is expressed as follows [39]:

$$\frac{t}{q_t} = \frac{1}{k_2 q_e^2} + \frac{1}{q_e t}$$

The plots of  $t/q_t$  versus  $t$  (Fig. 14) are straight lines where slopes and intercepts are respectively  $1/q_e$  and  $1/k_2 q_e^2$ . The rate constant  $k_2$  and the equilibrium sorption capacity  $q_e$  values are calculated from these parameters.

The Elovich model describes a number of reaction mechanisms including bulk and surface diffusion and deactivation of catalytic surfaces [40, 41].

**Table 2** Comparison of maximum sorption capacity of xLVB with other sorbents

Adsorbents	$q_{\max}$ ( $\text{mg g}^{-1}$ )	References
Orange peel xanthate	204.50	[13]
Symphoricarpus albus	62.16	[29]
Myriophyllum spicatum	53.87	[30]
Phaseolus vulgaris L	42.77	[31]
xLVB	33.22	In this study
Xanthated sawdust	31.1–41.4	[32]
Groundnut hull	31.54	[14]
Chaff	12.5	[33]
Waste beer yeast	5.72	[34]
Typha angustifolia	3.719	[35]
Cladonia furcata	12.3	[36]

It is represented as:

$$q_t = \frac{1}{\beta} \ln(\alpha\beta) + \frac{1}{\beta} \ln t$$

where  $\alpha$  ( $\text{mg g}^{-1} \text{min}^{-1}$ ) and  $\beta$  ( $\text{g mg}^{-1}$ ) are constants of the adsorption and are determined from plot in Fig. 15.

Intraparticle diffusion model (IPD model) is defined by the following equation [42]:

$$q_t = K_{id}t^{1/2} + C$$

where  $K_{id}$  ( $\text{mg g}^{-1} \text{min}^{-1/2}$ ) is the adsorption constant,  $C$  is the intercept and is determined from plot  $q_t$  versus  $t^{1/2}$

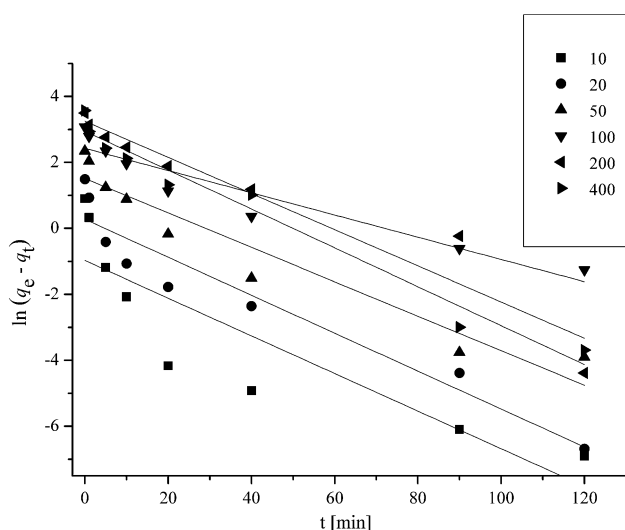


**Fig. 13** Pseudo-first-order plot for adsorption of Pb(II). Initial pH 5,  $[\text{Pb(II)}]_0 = 10.0, 20.0, 50.0, 100.0, 200.0, 400.0 \text{ mg dm}^{-3}$ , sorbent dose was  $4.0 \text{ g dm}^{-3}$ , temperature was  $25.0 \pm 0.5 \text{ }^\circ\text{C}$  and stirring speed 200 rpm

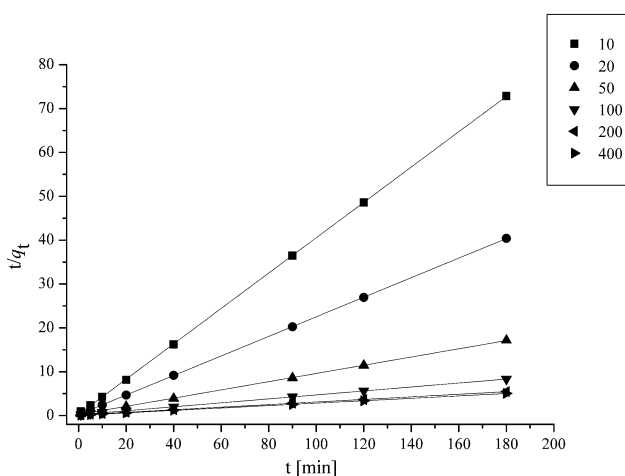


**Fig. 14** Pseudo-second-order plot for adsorption of Pb(II). Initial pH 5,  $[\text{Pb(II)}]_0 = 10.0, 20.0, 50.0, 100.0, 200.0, 400.0 \text{ mg dm}^{-3}$ , sorbent dose was  $4.0 \text{ g dm}^{-3}$ , temperature was  $25.0 \pm 0.5 \text{ }^\circ\text{C}$  and stirring speed 200 rpm

(Fig. 16). This model has been applied in three different forms:  $q_t$  is plotted against  $t^{1/2}$  to get a straight line that is forced to pass through the origin, multi-linearity plot  $q_t$  versus  $t^{1/2}$  and  $q_t$  is plotted against  $t^{1/2}$  to obtain a straight line but does not necessarily pass through the origin. The sorption process can be described by consecutive steps starting with liquid film diffusion, internal diffusion and sorption of solute on the interior surfaces of the pores of the sorbent.

The results of the kinetics parameters for Pb(II) ion, calculated from the linear plots of pseudo-first order and pseudo-second order kinetics models, as well as for

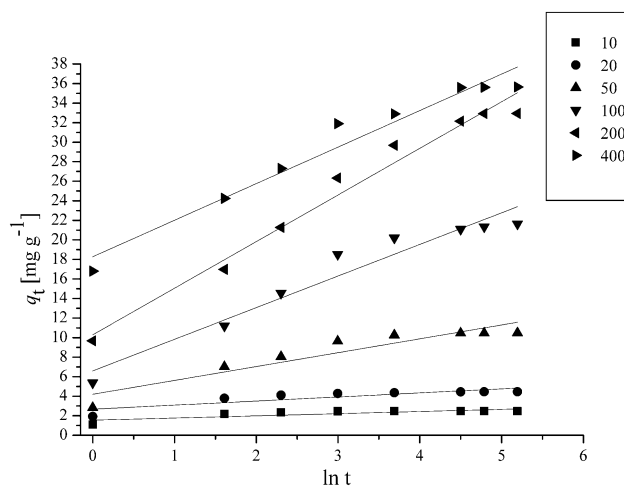


**Fig. 15** Elovich kinetic model for adsorption of Pb(II). Initial pH 5,  $[\text{Pb(II)}]_0 = 10.0, 20.0, 50.0, 100.0, 200.0, 400.0 \text{ mg dm}^{-3}$ , sorbent dose was  $4.0 \text{ g dm}^{-3}$ , temperature was  $25.0 \pm 0.5 \text{ }^\circ\text{C}$  and stirring speed 200 rpm

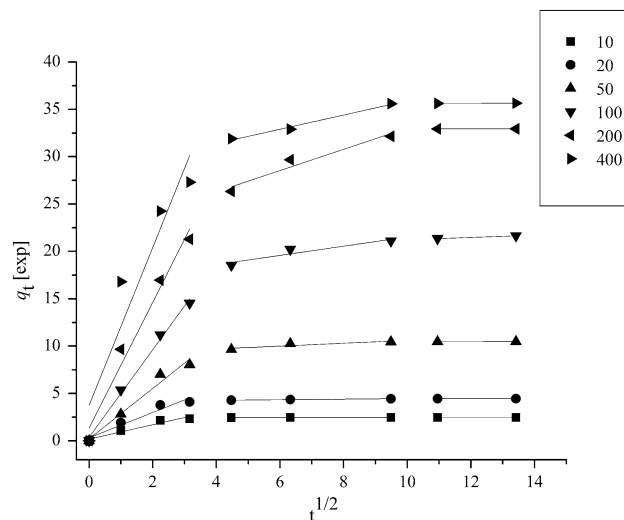


**Fig. 16** Intraparticle diffusion kinetic model for adsorption of Pb(II). Initial pH 5,  $[\text{Pb(II)}]_0 = 10.0, 20.0, 50.0, 100.0, 200.0, 400.0 \text{ mg dm}^{-3}$ , sorbent dose was  $4.0 \text{ g dm}^{-3}$ , temperature was  $25.0 \pm 0.5 \text{ }^\circ\text{C}$  and stirring speed 200 rpm

**Table 3** Comparison of experimental and calculated values for pseudo-first order, pseudo-second order, Elovich and intraparticle diffusion kinetic models rate constants

	10	20	50	100	200	400
$q_e^{\text{exp}}$	2.47025	4.455	10.4835	21.6322	32.9375	35.65
Pseudo-first order						
$k_1$	-0.05708	-0.05752	-0.05222	-0.0337	-0.05483	0.05896
$q_e^{\text{cal}}$	0.37729	1.31549	4.54465	11.3309	25.7831	19.0521
$r^2$	0.73953	0.911	0.90759	0.89432	0.91394	0.96663
Pseudo-second order						
$k_2$	0.6356	0.2199	0.0403	0.0107	0.0061	0.0109
$k_2^{\text{exp}}$	0.6415	0.2229	0.0403	0.0112	0.0065	0.0113
$q_e^{\text{cal}}$	2.4817	4.4847	10.6598	22.0848	33.9098	36.23
$r^2$	0.99997	0.99999	0.9999	0.99988	0.99961	0.99976
Elovich model						
$\alpha$	224.06	251.63	27.35	24.88	41.21	495.17
$\beta$	4.4857	2.3972	0.7043	0.309	0.2096	0.2673
$r^2$	0.62977	0.69603	0.85898	0.93517	0.97197	0.95051
Intraparticle diffusion model						
$K_{\text{id1}}$	0.76132	1.33335	2.66316	4.61788	6.63444	8.32968
$C_1$	0.18065	0.32469	0.21379	0.39143	1.36888	3.76345
$r^2$	0.91868	0.91769	0.96016	0.99116	0.96301	0.84036
$K_{\text{id2}}$	0.00253	0.03083	0.15204	0.48688	1.12073	0.75029
$C_2$	2.44482	4.15415	9.09336	16.64811	21.80753	28.39386
$r^2$	0.83607	0.96939	0.6434	0.79792	0.88959	0.97606

Elovich and intraparticle diffusion models are presented in Table 3 and Figs. 13, 14, 15 and 16.

The correlation coefficients,  $r^2$ , showed that the pseudo-second order model fits better with the experimental data than the pseudo-first order model. The pseudo-first order model shows the low correlation coefficient values  $0.7395 < r^2 < 0.9666$ , indicating that the pseudo-first-order model did not fit well to the experimental data (the initial concentration of lead ranging from 10.0 to 400.0 mg dm<sup>-3</sup>). The experimental data were observed to fit well to the pseudo-second order equation. The correlation coefficients ( $r^2$ ) for the linear plots of  $t/q_t$  against  $t$  for the pseudo-second order equation were observed to be close to 1 for Pb(II) ions. The theoretical  $q_e$  values for Pb(II) ions were also very close to the experimental  $q_e$  values. These observations suggest that metal sorption by xLVB followed the second-order reaction, which suggests that the process controlling the rate may be a chemical sorption involving valence forces through sharing or exchanging of electrons between sorbent and sorbate. Also, the mechanism of ion-exchange is probably involved, which is favored by the presence of xanthate groups with strong ion-exchange potential. The rate constant obtained through pseudo-second-order kinetic model varies inversely with increase in initial concentration which could be attributed to the lower competition for the sorption surface

sites at lower concentration. At higher concentrations, the competition for the surface active sites will be high and consequently lower sorption rates are obtained. Elovich kinetic model expresses the chemisorptions on heterogeneous solid surface active sites [43, 44]. In Elovich model  $\alpha$  is initial adsorption rate and is related to the rate of chemisorptions,  $\beta$  is desorption constant and is related to surface coverage [45]. The high value of constant  $\alpha$  suggests that a chemisorptions reaction took place and, by taking into account of  $\beta$  and  $r^2$  values, we can say that Elovich model can be fitted for experimental data.

The overall rate of adsorption can be described by the following three steps: first, the sharper portion is the external surface adsorption or instantaneous adsorption stage (slope  $K_{\text{id1}}$ ). The second portion is the gradual adsorption stage, where intraparticle diffusion is rate-controlled (slope  $K_{\text{id2}}$ ). The third portion is the final equilibrium stage where intraparticle diffusion starts to slow down due to extremely low adsorbate concentrations in the solution (slope  $K_{\text{id3}}$ ). The slowest of these steps controls the overall rate of the process. Fig. 16 depicts a plot of the intraparticle diffusion model kinetic model for the sorption of Pb(II). After stage 1 (0–10 min) follows the stage of intraparticle diffusion control (stage 2). Finally, in the third, final phase, after 90 min, intraparticle diffusion starts to slow down due to low Pb(II) ions concentration in the

solution [46]. The intraparticle diffusion model was utilized to determine the rate-limiting step of the sorption process. If the regression of  $q_t$  versus  $t^{1/2}$  is linear and passes through the origin, then intraparticle diffusion is the sole rate-limiting step [47]. The regression was linear, the plot did not pass through the origin, but was very close (Fig. 16) and it could be considered that both surface chemisorptions and intraparticle diffusion operated parallel during the xLVB sorption process. The value of rate constant for intraparticle diffusion  $K_{id1}$  and  $K_{id2}$  shown in Table 3 increases with increasing initial Pb(II) concentration. Increasing constant for intraparticle diffusion  $K_{id1}$  and  $K_{id2}$  indicates greater driving force with increasing initial Pb(II) concentration (bulk liquid concentration raises the driving force of Pb(II) to transfer from the bulk solution onto and into the solid particle). Based on  $K_{id1}$  and  $K_{id2}$  values it can be concluded that film diffusion is more efficient than intraparticle diffusion.

In addition, the  $C_1$  and  $C_2$  (thickness of the boundary layer) values varied like the  $K_{id}$  values with initial concentration (Table 3) indicating the film diffusion in the rate-limiting step. Larger  $C$  value corresponds to a greater boundary layer diffusion effect. The results of this study demonstrated increasing initial concentration which promoted the boundary layer diffusion effect, the contribution of the film diffusion in the rate-limiting step. The correlation coefficients for the intraparticle diffusion model are slightly lower than those of the pseudo-second-order kinetic model.

#### The battery industry wastewater

Lead is one of the vital ingredients of lead acid batteries. The growth of lead-acid battery production increase with the number of automotive vehicles. On the other hand, the maximum allowable concentration of lead is  $0.01 \text{ mg dm}^{-3}$  for drinking water (World Health Organization). Therefore, the concentration of this metal must be reduced to the level that satisfies environmental regulations for various types of water. The levels of pollutants in lead acid battery wastewater vary depending upon the type of process adopted in battery making. A recent survey of a battery factory showed that the pH of wastewater at the source was in range from 1.4 to 3.3, while the concentration of dissolved lead varies in the range from 5 to  $30 \text{ mg dm}^{-3}$  [48]. However, wastewater from battery factories contains multiple metals, which are likely to cause interactive effects depending on the number of metals competing for binding sites on xLVB. The composition of local battery factory wastewater in  $\text{mg dm}^{-3}$  was: 25.23 Pb, 11.70 Fe, 14.70 Zn, 710 sulfate, COD 458.2 and pH 3.1. To determine the dependence of metal sorption on xLVB, 4 g of xLVB was exposed to  $1.0 \text{ dm}^3$  of wastewater with pH adjusted to 5.0. Obtained removal efficiency of

Pb(II) ions was 95.7 %. The removal efficiency for Fe and Zn ions in the wastewater was about 90 %. The sorption of Pb(II) ions is a competitive process with sorption of Fe and Zn ions in solution. The factors that affect the binding of metal ions on xLVB largely depend on the physico-chemical properties of metals [34]. The results also reveal that the treatment of Pb(II) ions in wastewater samples is not significantly different from the results obtained in model conditions. About 4 % decrease in removal efficiency in the case of wastewater sample, compared to the synthetic sample, may be attributed to the presence of other metal ions in wastewater (Fe and Zn).

#### Conclusions

In this study the characteristics, important parameters that determine the process of heavy metal sorption and the possible sorption mechanism by xanthated *Lagenaria vulgaris* shell have been shown. The sorption of metal ions was dependent on such experimental conditions as pH, sorbate and sorbent concentrations and sorbate–sorbent contact time. Kinetic experiments proved that the biosorption process was rapid, with equilibrium achieved practically in  $< 40$  min. The pseudo-second-order kinetic model provides the best correlation of the experimental data, which suggests that the process controlling the rate may be a chemisorption and ion-exchange. The adsorption process can also be described by the three-stage intraparticle diffusion model, which indicates that both chemical and diffusion process were involved in the biosorption of Pb(II) ions onto xLVB. The obtained results showed that initial pH highly affected the uptake capacity of the biosorbent. For Pb(II) ions the optimal value of pH for biosorption was 5. The experimental data of adsorbing Pb(II) ions fit well to Langmuir model and the maximum adsorptive quantity of xLVB was  $33.21 \text{ mg g}^{-1}$ . FTIR spectra confirms the presence of the xanthate group on the xLVB and indicates that the functional groups, such as hydroxyl, carboxylic, C–S, C = S participated in the adsorption process for Pb(II) ions. EDX spectra of xLVB, before and after the metal sorption, further supported the hypothesis of the involvement of the ion-exchange mechanism. From the presented results, it may be concluded that biosorbent based on xanthated *Lagenaria vulgaris* shell had the potential to be used as an efficient, cost-effective and available means for the removal of Pb(II) ions from wastewater effluents. The regeneration and desorption aspect of xLVB needs further studies for its real cost effectiveness.

**Acknowledgments** Authors would like to acknowledge the financial support of the Ministry of Education, Science and Technological Development of the Republic of Serbia (Grants No TR34008 and III43009).

## References

1. R. Ansari, F. Raofile, E J Chem. **3**(1), 49 (2006)
2. A. Özer, J. Hazard. Mater. **141**, 753 (2007)
3. K.S. Hui, C.Y.H. Chao, S.C. Kot, J. Hazard. Mater. **127**, 89 (2005)
4. K.M. Miloš, R.D. Miljana, M.Z. Jelena, B.V. Danijela, M.D. Dragan, BLj Aleksandar, Hem. Ind. (2012). doi:10.2298/HEMIND120703097K
5. D. Sud, G. Mahajan, M.P. Kaur, Bioresour. Technol. **99**, 6017 (2008)
6. B. Deepak, L.H. Puspa, N.G. Kedar, J. Nepal Chem. Soc. **26**, 53 (2010)
7. G.I. Muhammad, S. Asma, I.Z. Saeed, J. Hazard. Mater. **164**, 161 (2009)
8. G.B. Carmen, B. Dominique, J.A.G. Richard, E.G. van Dam Jan, Ind. Crops Prod. **20**, 205 (2004)
9. K.V. Kumar, K. Porkodi, J. Hazard. Mater. **146**, 214 (2007)
10. A. Saeed, M.W. Akhter, M. Iqbal, Sep. Purif. Technol. **45**, 25 (2005)
11. N. Raziya, A.H. Muhammad, S. Fatima, P. Shahnaz, N.Z. Muhammad, I. Tahira, J. Hazard. Mater. **150**, 335 (2008)
12. P. Saueprasearsit, M. Nuanjaraen, M. Chinlapa, Environ Res J **4**, 157 (2010)
13. S. Liang, X. Guo, N. Feng, Q. Tian, J. Hazard. Mater. **170**, 425 (2009)
14. Q. Suleman, R. S. Anwar, U. Muhammad, Electron. J. Biotechnol. **12**, (2009)
15. I. Langmuir, J. Am. Chem. Soc. **40**, 1361 (1918)
16. H.M.F. Freundlich, J. Phys. Chem. **57**, 385 (1906)
17. M.I. Temkin, V. Pyzhev, Acta Physiochim. URSS **12**, 327 (1940)
18. M. Hosseini, S.F.L. Mertens, M. Ghorbani, M.R. Arshadi, Mater. Chem. Phys. **78**, 800 (2003)
19. M.M. Dubinin, L.V. Radushkevich, Proc. Acad. Sci. USSR **55**, 331 (1947)
20. M.M. Dubinin, Chem. Rev. **60**, 235 (1960)
21. J.P. Hobson, J. Phys. Chem. **73**, 2720 (1969)
22. S. Liang, X. Guo, N. Feng, Q. Tian, J. Hazard. Mater. **170**, 425 (2009)
23. B.E. Reed, M.R. Matsumoto, Sci. Technol. **28**, 2179 (1993)
24. G. McKay, M.S. Otterburn, A.G. Sweeney, Water Res. **14**, 15 (1980)
25. W.W. Enos, M.K. Gerald, K. Joseph, S.M. Paul, Bull. Chem. Soc. Ethiop. **25**, 181 (2011)
26. P. Lodeiro, J.L. Barriada, R. Herrero, M.E. Sastre de Vicente, Environ. Pollut. **142**, 264 (2006)
27. A. Sari, M. Tuzen, M. Soylak, J. Hazard. Mater. **144**, 41 (2007)
28. U. Shafique, A. Ijaz, M. Salman, W. Zaman, N. Jamil, R. Rehman, A. Javaid, J Taiwan Inst Chem Eng **43**, 256 (2012)
29. T.A. Sibel, G. Asli, A. Burcu, K. Zerrin, A. Tamer, J. Hazard. Mater. **165**, 126 (2009)
30. C. Yan, G. Li, P. Xue, Q. Wei, Q. Li, J. Hazard. Mater. **179**, 721 (2010)
31. A.S. Özcan, S. Tunali, T. Akar, A. Özcan, Desalination **244**, 188 (2009)
32. C.M. Flynn Jr, T.G. Carnahan, R.E. Lindstrom, *Adsorption of heavy metal ions by xanthate sawdust* (U.S. Dept. of the Interior, Bureau of Mines, Washington, 1980), pp. 1–11
33. R. Han, J. Zhang, W. Zou, J. Shi, H. Liu, J. Hazard. Mater. **125**, 266 (2005)
34. R. Han, H. Li, Y. Li, J. Zhang, H. Xiao, J. Shi, J. Hazard. Mater. **137**, 1569 (2006)
35. L.S.L. Yen, G.J. Collin, H. Siew-Eng, J. Serb. Chem. Soc. **76**, 1037 (2011)
36. S. Ahmet, T. Mustafa, D.U. Özgür, S. Mustafa, Biochem. Eng. J. **37**, 151 (2007)
37. A. Abdellah, S.O. Mohand, H.E. El, C.M. Louis, L. Marc, J. Hazard. Mater. **163**, 441 (2009)
38. Y.S. Ho, G. McKay, Can. J. Chem. Eng. **76**, 822 (1998)
39. Y.S. Ho, G. McKay, J. Process. Biochem. **34**, 451 (1999)
40. S.H. Chien, W.R. Clayton, Soil Sci. Soc. Am. J. **44**, 265 (1980)
41. C.W. Cheung, J.F. Porter, G. McKay, Sep. Purif. Technol. **19**, 55 (2000)
42. S. Altenor, B. Carene, E. Emmanuel, J. Lambert, J.J. Ehrhardt, S. Gaspard, J. Hazard. Mater. **165**, 1029 (2009)
43. L.L. Violeta, L.H. Susana, D.B. Carlos, N.U. Fernando, B. Bryan, J. Hazard. Mater. **161**, 1255 (2009)
44. A.B. Pérez Marín, M.I. Aguilar, V.F. Meseguer, J.F. Ortuño, J. Sáez, M. Lloréns, Chem. Eng. J. **155**, 199 (2009)
45. N. Raziya, N.H. Mubashir, H.S. Muhammad, Chem. Eng. J. **150**, 40 (2009)
46. C. Theivarasu, S. Mylsamy, Int J. Eng. Sci. Tech. **2**, 6284 (2010)
47. P.S. Kumar, R. Gayathri, J. Eng. Sci. Tech. **4**, 381 (2009)
48. S. Khaoya, U. Pancharoen, Int J Chem Eng Appl **3**, 98 (2012)